Diagnosing Cancer in Vivo

Frank Koenig, Joachim Knittel, Herbert Stepp

The modern era of medicine has seen the development of new instruments and analyses for examining the human body. Such advances have been accompanied by an increased life expectancy, but a by-product of longer life is a greater likelihood of developing cancer. Consequently, interest in improved noninvasive technologies for the diagnosis of cancer has been heightened. Excisional biopsies, which traditionally have been used to determine these parameters, pose numerous shortcomings for the patient, including bleeding, infection, or perforation from obtaining the tissue; complications from anesthesia; nonrepresentative biopsies, which miss the invasive part of a tumor and lead to an underestimate of tumor invasion; spread of the tumor cells through blood and lymphatic vessels, arising from mechanical agitation; and inability of standard visual analyses to differentiate flat malignant lesions from normal or inflamed tissue.

The three pieces of information sought about a cancer in vivo are its (i) location (detection), (ii) invasion (staging), and (iii) differentiation status (grading). Achieving these objectives requires wide-ranging methodologies. Tumor grading requires microscopic resolution. Staging necessitates a higher penetration depth to recognize tissue structures such as mucosa, submucosa, and muscle layer. Localizing malignant lesions may require scanning a large surface for flat, hardly visible malignancies, such as in the urinary bladder, lung, or intestine.

At present, no single instrument can replace excisional biopsies for obtaining information. However, numerous instruments and computer-based analyses are under rapid development to improve data collection. Although the techniques described in this article might be effectively employed in numerous organs of the body, we illustrate here the application of these techniques primarily for the detection, staging, and grading of tumors in the urinary bladder.

Techniques for detection, or localization, of tumors include the use of endoscopes for hollow organs of the body (e.g., bladder, colon, esophagus) and x-rays, magnetic resonance imaging (MRI), or ultrasound for less accessible parts of the body. Although state-of-the-art endoscopy allows high-resolution imaging of the entire bladder surface, flat lesions including the highly malignant carcinoma in situ (CIS) may still be missed. This leads to tumor recurrence, and some of these undetected lesions may progress to invasive carcinomas. The overall recurrence rate of bladder carcinoma is between 30 and 70% and is related to the primary tumor grade and stage, as well as to the number of tumors initially removed (*1*).

To improve the detection of dysplastic and malignant lesions, including CIS, several research groups are using 5-aminolevulinic acid (ALA) to improve the diagnosis of bladder carcinomas (*2–4*). ALA is a nonfluorescent precursor of fluorescent protoporphyrin IX (PPIX) that has been shown to accumulate in a variety of malignancies, whereas surrounding normal tissue shows no or considerably less PPIX. The mechanisms by which tumor cells are preferentially stained by PPIX are not fully understood, but they may involve a higher cellular uptake of ALA through an active transport mechanism and a disturbed efflux of PPIX.

For photodetection of bladder carcinoma, an ALA solution is instilled intravesically before endoscopy. The tumor-selective buildup of PPIX enables high-contrast imaging, revealing flat or micro-papillary malignant lesions of the bladder not otherwise detectable. The endoscopic equipment for the detection of PPIX-fluorescence is already commercially available.

A nonexcisional staging method currently in experimental use is intravesical ultrasound. The use of high-frequency ultrasound in combination with miniature (2 mm) scanning probes in an endoscope allows in vivo diagnosis of T2 (muscle-invasive) urothelial carcinoma (*5*, *6*). A disadvantage of ultrasound is that its resolution (250 to 500 μm) is not sufficient to distinguish Ta (epithelial) from T1 (lamina propria) tumors.

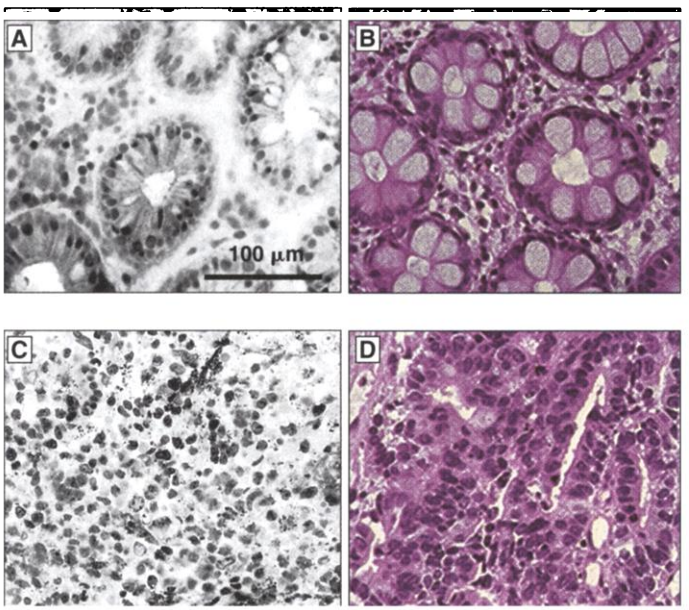

Images of the human colon. CLSM (10 μm below the surface) versus standard histological photomicrograph for normal colonic tissue (**A** and **B**) and colonic carcinoma (**C** and **D**).

A recently described method, optical coherence tomography (OCT), supersedes ultrasound in some regards. It allows cross-sectional imaging of tissue microstructures to 4 mm in depth with a spatial resolution of ~10 μm, about 25 times higher than the resolution of ultrasound (*7*). OCT also differs in its use of reflected infrared light rather than acoustical waves. OCT uses light with a short coherence length, which is delivered by a luminescence diode or a short-pulse laser. Cross-sectional tomographic images are produced by scanning the light beam across the surface of target tissues. An interferometer is used to measure the depth inside the tissue from where light is scattered back. Combined with optical fiber components and integrated with conventional endoscopes, ex vivo and in vivo OCT imaging has been studied on several tissue types, e.g., respiratory tract, intestine, skin, vessels, and eye (*8*). These studies, as well as ex vivo studies on urologic tissue (prostate, ureter, bladder), have shown that OCT effec-

F. K. is in the Department of Urology, Charité Medical School, Humboldt University Berlin, Germany (frank.koenig@charite.de). J. K. is in the Department of Minimally Invasive Surgery (MIC), University Tuebingen, Germany. H. S. is in the Laser-Forschungslabor, Department of Urology, Clinics of the University of Munich-Grosshadern, Germany.

tively reveals architectural tissue morphology without requiring excisional biopsy (*9*). OCT may have the potential to differentiate between flat malignant and inflammatory lesions. In addition, it is hoped that muscle invasion of malignancies may also be determined.

Determination of the differentiation state of tumor cells is routinely performed by a pathologist on biopsy samples or surgically removed tissue. Parameters for grading include cellular shape and size, chromatin appearance, prominent nucleoli, mitotic figures, and the nuclear-to-cytoplasmic ratio. In vivo confocal laser scanning microscopy (CLSM) can provide much of this information (*10*, *11*). With CLSM, cell structures and structural morphologic features can be visualized from thin "sections" within living tissue, to maximal depths of 200 to 500 μm, a lateral resolution of 0.5 to 1 μm, and an axial resolution of 3 to 5 μm. As shown for the colon (see both figures), fluorescent markers can further enhance the quality of CLSM images staining cell structures like membranes, the nucleus, or nucleoli. For analyses on a smaller scale, fiber-optic imaging bundles or miniaturized microscopes may eventually enable endoscopic microscopy (*12*–*16*). Images suitable for diagnostic purposes can be transmitted via a fiber-optic imaging bundle (see figure, this page). The diameter of the active area is 720 μm, and the circular field of view (image size) is 180 μm. Recently, a miniaturized version of such a microscope with an outer diameter below 2 mm was developed. It can be introduced into the human body through the working channel of a standard fiber endoscope. The resolution of this first prototype is about 3.1 μm but will be improved (*17*). In the near future, endoscopic microscopy may be improved by using probes with 50,000 or even 100,000 single optical fibers and by reducing the aberrations of the optical system.

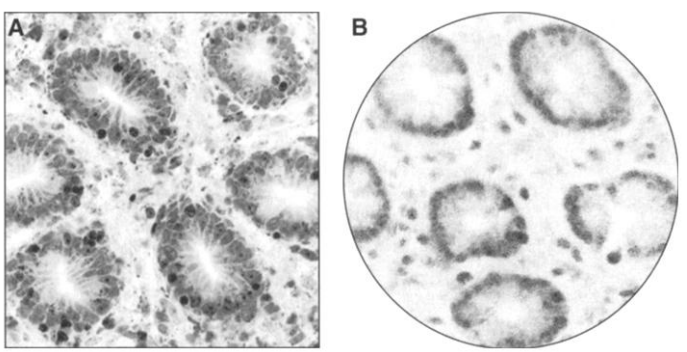

Through a fiber bundle. (**A**) CLSM image of a normal colonic tissue. (**B**) Corresponding image obtained through a bundle of 30,000 single fibers.

Ultrasound, OCT, and CSLM are useful for imaging tissue in a way previously not accessible with endoscopy. Extracting and interpreting relevant information for staging and grading currently requires a trained human being. For fully automated endoscopic pathological diagnoses, sophisticated image analysis software will be needed. Steps in image processing for peforming automated biopsies include (i) detection of possible tumors by outlining of PPIX-fluorescence positive areas, (ii) assessment of staging from calculation of tumor penetration depth from ultrasound or OCT images, and (iii) grading of tumors through classification of morphological features on a cellular level in confocal images.

Outlining is straightforward because fluorescence can be captured by color CCD cameras. Suspicious areas are characterized by a certain hue that can easily be determined independent of observation distance, angle, or variation of optical tissue parameters (*18*). Therefore, it is possible to automatically demarcate areas of predetermined hue values, thus indicating the presence of suspicious tissue.

Analysis of OCT images provides two-dimensional cross-sectional imaging of tissue and information about staging. Automated contour detection techniques that enable quantitation of different blood vessel parameters have already been developed for intravascular ultrasound (*19*, *20*). Automated tumor staging on OCT images using similar segmentation algorithms appears feasible.

CLSM image analysis may allow grading and thus be able to differentiate between benign and malignant tissue. This currently requires the expertise of a histopathologist. Automated histological classification of cell material obtained from the cervix (*21*, *22*), or the tracheobronchial system (*23*), and prostate tissue sections (*24*) has been performed with favorable results. However, the established algorithms were applied to color images of biopsied tissue taken through a microscope and required prior cell staining. Endoscopic CLSM images, on the other hand, are primarily grayscale and will hardly be able to provide as much contrast as stained cytology specimens. Therefore, the search for contrast-enhancing markers that can be applied clinically will be one of the major challenges for the development of a multisensor optical biopsy device. In principle, two possibilities exist to extract relevant information from CLSM images. First, one could incorporate objective decision criteria of experienced histopathologists into the software. This approach typically starts with the segmentation of an image into different types of objects: tissue layers, vessels, cells, nuclei, etc. Then, parameters such as the nuclear-to-cytoplasmic ratio are calculated, resulting in a "probability of malignancy" score. An alternative route would be to extract more abstract image parameters on the basis of gray level and then analyze the structure. Neural network-like algorithms can separate important from less-important image parameters, also ultimately yielding a malignancy probability.

We think automated endoscopic in vivo diagnosis of cancer is a realistic goal that, when accomplished, will benefit the diagnosis and treatment of diseased tissue. Real-time, in vivo analysis eliminates artifacts caused by biopsy forceps, cautery, and fixation or staining procedures. In contrast to traditional white light endoscopy, which allows imaging of only two-dimensional surfaces, the combination of OCT, ultrasound, and endoscopic CLSM may enable three-dimensional high-resolution imaging at shallow depth. In addition, the cost of performing histological studies on excised tissue is a significant expense in hospitals, which optical techniques could reduce by decreasing the number of biopsies or replacing them altogether. Through automation of the diagnostic process, cancer screening could become less time consuming, less invasive, and highly efficient at a lowered expense.

References and Notes

1. L. A. Kiemeney *et al.*, *J. Urol.* **150**, 60 (1993).
2. M. Kriegmair *et al.*, *J. Urol.* **155**, 105 (1996).
3. P. Jichlinski *et al.*, *Laser Surg. Med.* **20**, 402 (1997).
4. F. Koenig *et al.*, *Br. J. Urol.* **83**, 129 (1999).
5. M. Koraitim, B. Kamal, N. Metwalli, Y. Zaky, *J. Urol.* **154**, 375 (1995).
6. K. Uchida, H. Akaza, *Endoscopy* **30**, A14 (1998).
7. D. A. Benaron, W. F. Cheong, D. K. Stevenson, *Science* **276**, 2002 (1997).
8. G. J. Tearney *et al.*, *Science* **276**, 2037 (1997).
9. G. J. Tearney *et al.*, *J. Urol.* **157**, 1915 (1997).
10. M. Rajadhyaksha *et al.*, *J. Invest. Dermatol.* **104**, 946 (1995).
11. F. Koenig *et al.*, *Urology* **53**, 853 (1999).
12. T. Dabbs, M. Glass, *Appl. Opt.* **31**, 3030 (1992).
13. A. F. Gmitro, D. Aziz, *Opt. Lett.* **18**, 565 (1993).
14. G. J. Tearney, R. H. Webb, B. E. Bouma, *Opt. Lett.* **23**, 1152 (1998).
15. D. L. Dickensheets, G. S. Kino, *Opt. Lett.* **21**, 764 (1996).
16. ———, *J. Microelectromech. Syst.* **7**, 38 (1998).
17. J. Knittel *et al.*, *Opt. Com.*, **188**, 267 (2001).
18. H. Stepp *et al.*, *Proc. SPIE* **2627**, 13 (1995).
19. J. Dijkstra, G. Koning, J. H. Reiber, *Int. J. Card. Imaging* **15**, 513 (1999).
20. N. Bom *et al.*, *Eur. J. Ultrasound* **7**, 9 (1998).
21. O. Abulafia, D. M. Sherer, *Obstet. Gynecol. Surv.* **54**, 253 (1999).
22. M. Spitzer, *Am. J. Obstet. Gynecol.* **179**, 544 (1998).
23. N. Ikeda *et al.*, *Lung-Cancer* **19**, 61 (1998).
24. P. W. Hamilton *et al.*, *Anal. Quant. Cytol. Histol.* **20**, 443 (1998).
25. We thank B. Bültmann and U. Vogel for their support and providing access to the CLSM, and T. Deutsch for helpful discussions. We also thank H. Raestrup, M. Wehrmann, A. Greschniok, and P. Ruck for supplying the tissue samples, and M. Lein for help and support with the animal model.